



ELSEVIER

Available online at [www.sciencedirect.com](http://www.sciencedirect.com)

SCIENCE @ DIRECT®

NUCLEAR  
PHYSICS A

Nuclear Physics A 717 (2003) 129–145

[www.elsevier.com/locate/npe](http://www.elsevier.com/locate/npe)

## Two-neutrino $2\beta$ decay of $^{116}\text{Cd}$ and new half-life limits on $2\beta$ decay of $^{180}\text{W}$ and $^{186}\text{W}$

F.A. Danevich<sup>a</sup>, A.Sh. Georgadze<sup>a</sup>, V.V. Kobychiev<sup>a,1</sup>,  
A.S. Nikolaiko<sup>a</sup>, O.A. Ponkratenko<sup>a</sup>, V.I. Tretyak<sup>a</sup>,  
S.Yu. Zdesenko<sup>a</sup>, Yu.G. Zdesenko<sup>a,\*</sup>, P.G. Bizzeti<sup>b</sup>,  
T.F. Fazzini<sup>b</sup>, P.R. Maurenzig<sup>b</sup>

<sup>a</sup> *Institute for Nuclear Research, MSP 03680 Kiev, Ukraine*

<sup>b</sup> *Dipartimento di Fisica, Università di Firenze and INFN, 50019 Firenze, Italy*

Received 27 September 2002; received in revised form 3 December 2002; accepted 7 January 2003

### Abstract

Studies of the  $2\beta$  decay of  $^{116}\text{Cd}$ ,  $^{180}\text{W}$  and  $^{186}\text{W}$  have been performed in the Solotvina Underground Laboratory with the help of the super-low background  $^{116}\text{CdWO}_4$  crystal scintillators. The half-life value of the two-neutrino  $2\beta$  decay of  $^{116}\text{Cd}$  has been revised as

$$T_{1/2}^{2\nu} = 2.9 \pm 0.1(\text{stat})_{-0.3}^{+0.4}(\text{syst}) \times 10^{19} \text{ yr.}$$

Besides, the new half-life limits on different modes of this process have been established for two natural tungsten isotopes, in particular,  $T_{1/2} \geq 1.0$  ( $1.6$ )  $\times 10^{21}$  yr at 90% (68%) C.L. for the neutrinoless  $2\beta$  decay of  $^{186}\text{W}$  to the ground ( $0^+$ ) and first excited ( $2^+$ ) level of  $^{186}\text{Os}$ .

© 2003 Elsevier Science B.V. All rights reserved.

PACS: 23.40.-s; 27.60.+g; 29.40.Mc

Keywords: Double beta decay;  $^{116}\text{Cd}$ ;  $^{180}\text{W}$ ;  $^{186}\text{W}$ ;  $\text{CdWO}_4$  crystal scintillators

\* Corresponding author.

E-mail address: [zdesenko@kinr.kiev.ua](mailto:zdesenko@kinr.kiev.ua) (Yu.G. Zdesenko).

<sup>1</sup> Current address: INFN, Laboratori Nazionali del Gran Sasso, 67010 Assergi (AQ), Italy.

## 1. Introduction

Recent observations of neutrino oscillations [1–3] provide important motivation for double beta ( $2\beta$ ) decay experiments [4–6]. Indeed, neutrinoless ( $0\nu$ ) mode of  $2\beta$  decay, which violates lepton number ( $L$ ) conservation and requires neutrino to be a massive Majorana particle, is forbidden in the framework of the standard model (SM) of electroweak theory. However, many extensions of the SM incorporate  $L$  violating interactions and, thus, could lead to this process, which when observed, will prove the Majorana nature of the neutrino. Moreover, while oscillation experiments are sensitive to the neutrino mass difference, only the measured  $0\nu 2\beta$  decay rate can give the absolute scale of the effective Majorana neutrino mass and, consequently, could test different neutrino mixing models. Hence, the discovery of the  $0\nu 2\beta$  decay would be a clear evidence for a new physics beyond the SM [4–6].

Despite numerous experimental efforts this process still remains unobserved, and only half-life limits for  $0\nu$  mode were obtained in direct experiments up to now (see reviews [4–7]). The highest bounds were established for several nuclides:  $T_{1/2}^{0\nu} \geq 10^{21}$  yr for  $^{48}\text{Ca}$  [8],  $^{150}\text{Nd}$  [9],  $^{160}\text{Gd}$  [10];  $T_{1/2}^{0\nu} \geq 10^{22}$  yr for  $^{82}\text{Se}$  [11],  $^{100}\text{Mo}$  [12];  $T_{1/2}^{0\nu} \geq 10^{23}$  yr for  $^{116}\text{Cd}$  [13],  $^{128}\text{Te}$ ,  $^{130}\text{Te}$  [14],  $^{136}\text{Xe}$  [15]; and  $T_{1/2}^{0\nu} \geq 10^{25}$  yr for  $^{76}\text{Ge}$  [16,17].

In this paper the revised  $T_{1/2}^{2\nu}$  value of the two-neutrino  $2\beta$  decay of  $^{116}\text{Cd}$  (determined with a greater accuracy) and results of the search for the double beta decay processes in  $^{180}\text{W}$  and  $^{186}\text{W}$  nuclei are presented. They were obtained by analyzing the data ( $\approx 0.5$  yr kg statistics) collected in the course of the Solotvina  $2\beta$  decay experiment on  $^{116}\text{Cd}$  with the help of low-background cadmium tungstate ( $\text{CdWO}_4$ ) crystal scintillators [13]. These crystals are enriched in  $^{116}\text{Cd}$  to 83%, and, hence, they can serve as source and detector of  $2\beta$  decay events simultaneously (so-called an “active” source technique).

The level scheme of the  $^{116}\text{Cd}$ – $^{116}\text{In}$ – $^{116}\text{Sn}$  triplet is depicted in Fig. 1(a), while the response functions of the  $^{116}\text{CdWO}_4$  detector for the different  $2\nu$  and  $0\nu$  modes of  $^{116}\text{Cd}$   $2\beta$  decay (simulated with the help of GEANT3.21 code [18] and event generator DECAY4 [19]) are shown in Fig. 1(b).

Besides,  $^{116}\text{CdWO}_4$  crystals contain two potentially  $2\beta$  decaying tungsten isotopes, whose abundance,  $\delta$ , are 0.12% for  $^{180}\text{W}$  and 28.4% for  $^{186}\text{W}$  [20]. The level scheme of the  $^{186}\text{W}$ – $^{186}\text{Re}$ – $^{186}\text{Os}$  triplet is depicted in Fig. 2(a), from which one can see that  $2\beta$  decay of  $^{186}\text{W}$  to the ground and excited  $2^+$  levels of  $^{186}\text{Os}$  is allowed energetically. If neutrinoless  $2\beta$  decays occur in the  $^{116}\text{CdWO}_4$  crystal, the peak at the energy  $Q_{\beta\beta} = 488$  keV [21] ( $Q_{2\beta}$  is the  $2\beta$  decay energy release) would be observed in the background spectrum of the detector (the width of peak is determined by the actual energy resolution of the latter). The sum electron spectrum of the two-neutrino  $2\beta$  decay of  $^{186}\text{W}$  should be a continuous distribution ending near  $Q_{\beta\beta}$  value. The response functions of the  $^{116}\text{CdWO}_4$  detector for the different  $2\beta$  decay modes of  $^{186}\text{W}$  (including  $0\nu$  transition with emission of a light neutral boson–Majoron– $0\nu 2\beta\text{M}$ ) are presented in Fig. 2(b)—they were also simulated with the help of the GEANT and DECAY4 codes.

Similarly, in accordance with the level scheme of the  $^{180}\text{W}$ – $^{180}\text{Ta}$ – $^{180}\text{Hf}$  triplet (see Fig. 3(a)), the double electron capture ( $2\varepsilon$ ) of  $^{180}\text{W}$  ( $Q_{2\varepsilon} = 146$  keV [21]) is allowed. In case of  $2\nu$  double electron capture from  $K$  shell ( $2\nu 2K$ ), the total energy released in a

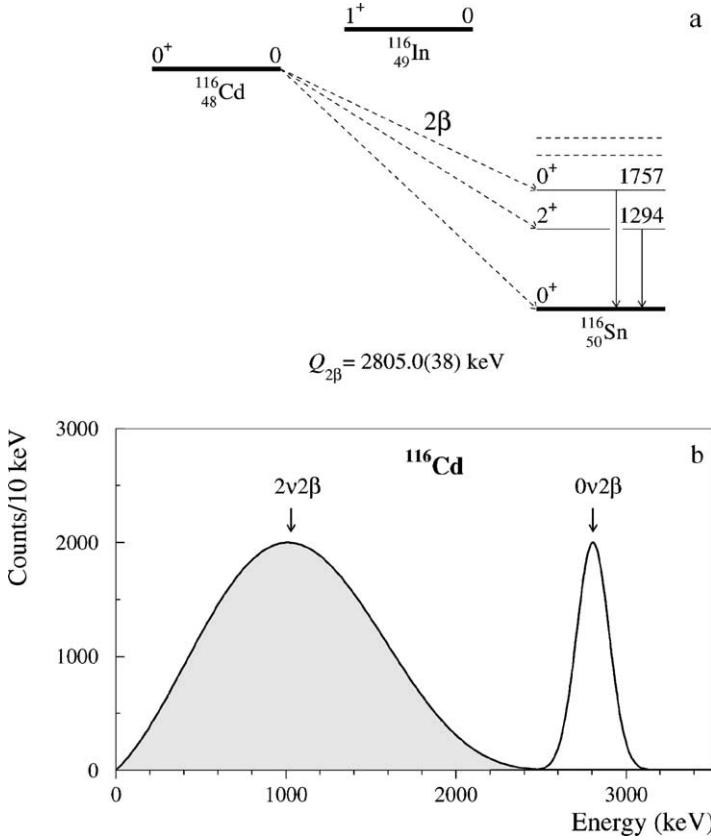


Fig. 1. (a) The scheme of the  $^{116}\text{Cd}$ - $^{116}\text{In}$ - $^{116}\text{Sn}$  triplet. The  $Q_{\beta\beta}$  energy is taken from [21]. (b) Simulated response functions of the  $^{116}\text{CdWO}_4$  crystal scintillators to the  $2\nu$  and  $0\nu$  modes of the  $2\beta$  decay of  $^{116}\text{Cd}$ .

detector is equal to  $2E_K$  (where  $E_K = 65.4$  keV is the binding energy of electrons on  $K$  shell of hafnium atom), while the rest of the energy ( $Q_{2\varepsilon} - 2E_K \approx 25$  keV) is carried away by neutrinos. For the neutrinoless double electron capture ( $0\nu 2\varepsilon$ ) all available energy (transferred to X-rays/auget electrons, gamma quanta or conversion electrons) will result in the peak at  $Q_{2\varepsilon} = 146$  keV value. The simulated response functions of the  $^{116}\text{CdWO}_4$  detector for the both modes are presented in Fig. 3(b).

## 2. Experiment

The description of the set-up with the cadmium tungstate ( $\text{CdWO}_4$ ) crystal scintillators and its performance have been published elsewhere (see for details [13] and references therein), thus only the main features of this apparatus are briefly summarized here. The experiment was carried out in the Solotvina Underground Laboratory at a depth of 1000 m of water equivalent [22]. Four  $^{116}\text{CdWO}_4$  crystals (enriched in  $^{116}\text{Cd}$  to 83%) with a total mass of 330 g were used. They are viewed by the low background 5'' EMI D724KFL

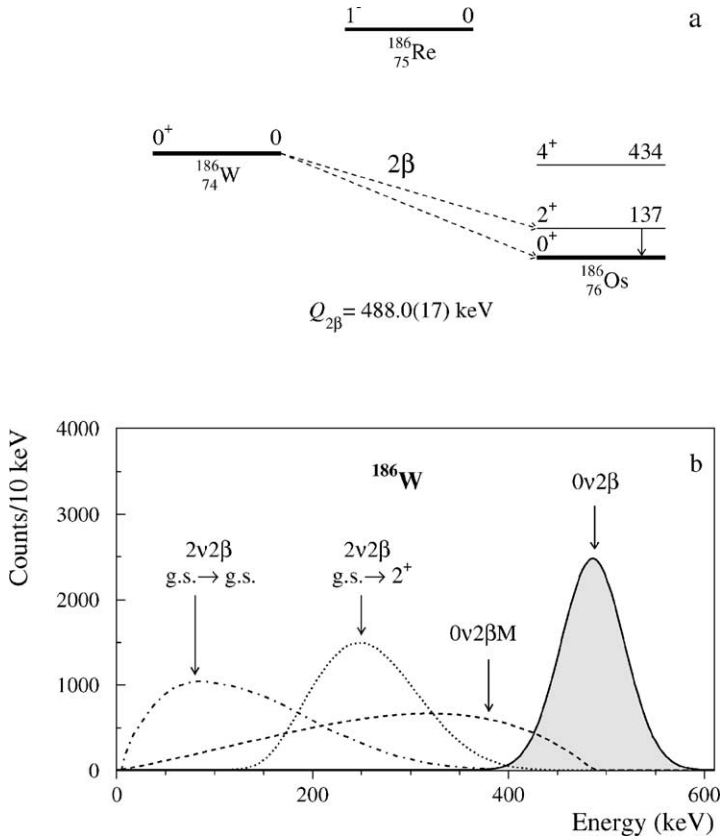


Fig. 2. (a) The scheme of the  $^{186}\text{W}$ - $^{186}\text{Re}$ - $^{186}\text{Os}$  triplet. (b) Simulated response functions of the  $^{116}\text{CdWO}_4$  crystal scintillators to the different modes of the  $2\beta$  decay of  $^{186}\text{W}$ . Due to high detection efficiency of  $^{116}\text{CdWO}_4$  scintillators to  $\gamma$  quanta with the energy 137 keV, response function for the  $0\nu 2\beta$  transition of  $^{186}\text{W}$  to the first excited level of  $^{186}\text{Os}$  is practically the same as for the  $0\nu 2\beta$  decay to the ground state.

photomultiplier (PMT) through one light guide 10 cm in diameter and 55 cm long. The light-guide is glued of two parts: high purity quartz (25 cm) and plastic scintillator (30 cm). The  $^{116}\text{CdWO}_4$  crystals are surrounded by an active shield made of 15 natural  $\text{CdWO}_4$  crystals with a total mass 20.6 kg. These are viewed by the low background PMT through an active plastic light guide  $\varnothing 17 \times 49$  cm. The whole  $\text{CdWO}_4$  array is situated within an additional active shield made of plastic scintillator  $40 \times 40 \times 95$  cm<sup>3</sup>, thus, together with both active light-guides, a complete  $4\pi$  active shield of the main ( $^{116}\text{CdWO}_4$ ) detector is provided. The outer passive shield consists of high purity copper (3–6 cm), lead (22.5–30 cm) and polyethylene (16 cm). Two plastic scintillators ( $120 \times 130 \times 3$  cm<sup>3</sup>) installed above the passive shield serve as cosmic muon veto.

An event-by-event data acquisition records the amplitude, arrival time, additional tags (the coincidence between main and shielding detectors) and pulse shape (in 2048 channels with 50 ns/channel) of events in the  $^{116}\text{CdWO}_4$  detectors in the energy range of 0.3–5 MeV. In the special runs the energy threshold was set at the level of 80 keV.

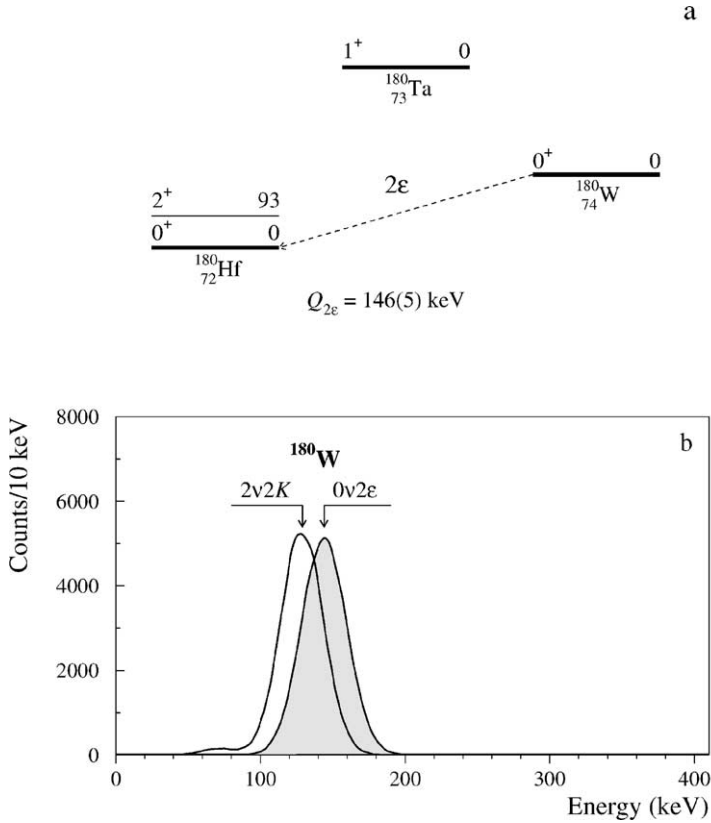


Fig. 3. (a) The scheme of the  $^{180}\text{W}$ - $^{180}\text{Ta}$ - $^{180}\text{Hf}$  triplet. (b) Simulated response functions of the  $^{116}\text{CdWO}_4$  crystals to the different modes of the double electron capture in  $^{180}\text{W}$ .

The energy scale and resolution of the detector were measured with  $\gamma$  sources in the energy range  $E_\gamma = (60\text{--}2615)$  keV. The energy dependence of the resolution is expressed as follows:  $\text{FWHM}_\gamma = -44 + \sqrt{2800 + 23.4E_\gamma}$ , where energy  $E_\gamma$  and  $\text{FWHM}_\gamma$  are in keV. For instance, energy resolution of 33.7%, 13.5% and 8.0% was obtained for 60 keV ( $^{241}\text{Am}$ ), 662 keV ( $^{137}\text{Cs}$ ) and 2615 keV ( $^{208}\text{Tl}$ )  $\gamma$  lines, respectively. The routine calibrations were carried out with  $^{207}\text{Bi}$  and  $^{232}\text{Th}$   $\gamma$  sources.<sup>2</sup> The dead time of the detector and acquisition was permanently controlled with the help of a light emitting diode optically connected to the main PMT (typical value was about 5%).

Also, the relative light yield for  $\alpha$  particles as compared with that for electrons ( $\alpha/\beta$  ratio) was determined in the energy range of 2.1–8.8 MeV:  $\alpha/\beta = 0.083 + 0.0168E_\alpha$ ,

<sup>2</sup> The stability of the spectrometer as a whole is proved by fact that the resolution of the  $^{137}\text{Cs}$  peak in the background spectra (collected over 13316 hours) is  $\text{FWHM} \approx 12\%$ , that is practically the same as measured in the calibration runs.

where  $E_\alpha$  is energy of  $\alpha$  particles in MeV (we refer to work [23], where response of the  $^{116}\text{CdWO}_4$  scintillators to  $\alpha$  particles has been studied).

According to the measured  $\alpha/\beta$  ratio, alpha particles from uranium and thorium trace contamination of the crystals can produce background in the 0.4–1.3 MeV energy region, where the peak of  $0\nu 2\beta$  decay of  $^{186}\text{W}$  is expected. To suppress such a background caused by  $\alpha$  particles, a method of pulse shape analysis (PSA) of  $\text{CdWO}_4$  scintillation signals, based on the optimal digital filter [24], was developed [23,25]. In the data processing the digital filter was applied to each experimental signal  $f(t)$  with aim to obtain the numerical characteristic of its shape (shape indicator, SI) defined as  $\text{SI} = \sum f(t_k) \times P(t_k) / \sum f(t_k)$ , where the sum is over time channels  $k$ , starting from the origin of signal and up to 75  $\mu\text{s}$ ,  $f(t_k)$  is the digitized amplitude (at the time  $t_k$ ) of a given signal. The weight function  $P(t)$  is defined as:  $P(t) = \{\bar{f}_\alpha(t) - \bar{f}_\gamma(t)\} / \{\bar{f}_\alpha(t) + \bar{f}_\gamma(t)\}$ , where  $\bar{f}_\alpha(t)$  and  $\bar{f}_\gamma(t)$  are the reference pulse shapes for  $\alpha$  particles and  $\gamma$  quanta, resulting from the average of a large number of experimental pulse shapes.

The energy dependence of the SI for  $\gamma$  quanta (electrons) was determined in the energy range of 80–2000 keV by using the data of the calibration measurements. We find linear dependence on energy for the 260–2000 keV gamma quanta:  $\text{SI}_\gamma = 0.29 - 0.71 \times 10^{-3} E_\gamma$ , and more rapid decreasing function in the energy range of 80–260 keV:  $\text{SI}_\gamma = 6.0 - 0.046 E_\gamma + 0.92 \times 10^{-4} E_\gamma^2$ .<sup>3</sup> The SI distributions measured with  $\alpha$  and  $\gamma$  sources are shown in Fig. 4(a). They are well described by Gaussian functions, whose standard deviations  $\sigma(\text{SI}_\alpha)$  and  $\sigma(\text{SI}_\gamma)$  depend on energy; in particular, for  $\gamma$  quanta  $\sigma(\text{SI}_\gamma) = 102 \cdot (E_\gamma)^{-1/2}$ , where  $E_\gamma$  is in keV. As it is seen from Fig. 4(a), the PSA technique allows us to distinguish clearly between electrons ( $\gamma$  rays) and  $\alpha$  particles emitted by sources. It is also true for the background events collected in the experiment. The SI distributions for such events measured during 4856 h with the PSA energy threshold of 300 keV in the energy interval 450–550 keV (it is the region of the  $0\nu 2\beta$  decay peak of  $^{186}\text{W}$ ) is depicted in Fig. 4(b). It is visible from this figure, that with the proper cut (e.g.,  $\text{SI} \leq 12$ ) the contribution of  $\alpha$  particles from the U/Th chains into the  $\gamma(\beta)$  spectrum is negligible (less than 0.5%). An illustration of the PSA of the background events is presented in Fig. 5 as three-dimensional distribution of the background events versus energy and shape indicator. In this plot one can see two clearly separated populations: the  $\alpha$  events, which belong to U/Th families, and  $\gamma(\beta)$  events.

The energy and arrival time of each measured event were used for analysis and selection of some decay chains in  $^{232}\text{Th}$ ,  $^{235}\text{U}$  and  $^{238}\text{U}$  families with aim to delete them from the background spectrum (see for details [13,26]). For instance, the following sequence of  $\alpha$  decays from the  $^{232}\text{Th}$  family was searched for and observed:  $^{224}\text{Ra}$  ( $Q_\alpha = 5.79$  MeV,  $T_{1/2} = 3.66$  d)  $\rightarrow$   $^{220}\text{Rn}$  ( $Q_\alpha = 6.40$  MeV,  $T_{1/2} = 55.6$  s)  $\rightarrow$   $^{216}\text{Po}$  ( $Q_\alpha = 6.91$  MeV,  $T_{1/2} = 0.145$  s)  $\rightarrow$   $^{212}\text{Pb}$ . The obtained  $\alpha$  peaks ( $\alpha$  nature of events was confirmed by the PSA described above), as well as the distributions of the time intervals between events are

<sup>3</sup> Here all variables are dimensionless, and  $E_\gamma$  is expressed in keV.

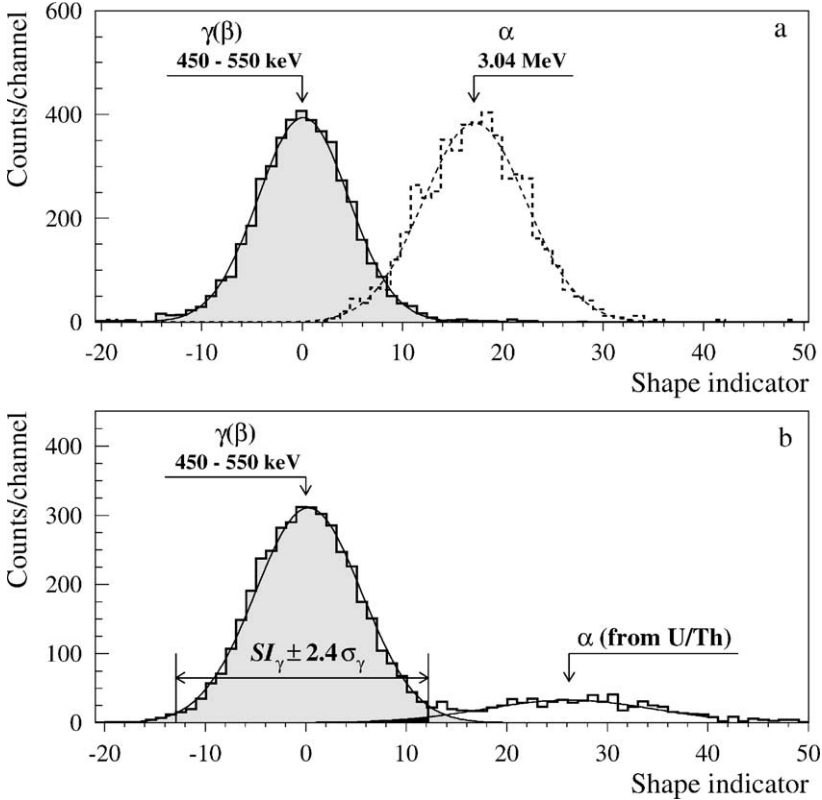


Fig. 4. (a) The shape indicator (SI) distributions measured by the enriched  $^{116}\text{CdWO}_4$  crystal ( $\varnothing 32 \times 19$  mm) with  $\alpha$  particles ( $E_\alpha = 3.04$  MeV) and  $\gamma$  rays ( $E_\gamma = 450\text{--}550$  keV). (b) The SI distributions for the background events measured (4856 h) by the  $^{116}\text{CdWO}_4$  crystals in the energy interval 450–550 keV. The part of the  $\text{SI}_\alpha$  distribution, which contributes to the  $\gamma(\beta)$  spectrum (within the  $\pm 2.4\sigma_\gamma$  interval of  $\text{SI}_\gamma$ ), is less than 0.5% (filled in black).

in a good agreement with those expected for  $\alpha$  particles of  $^{224}\text{Ra}$ ,  $^{220}\text{Rn}$  and  $^{216}\text{Po}$ . On this basis the activity of  $^{228}\text{Th}$  in  $^{116}\text{CdWO}_4$  crystals was determined as  $39(2)$   $\mu\text{Bq/kg}$ .<sup>4</sup>

Due to active and passive shields of the set-up, and as a result of the time-amplitude and pulse-shape analysis of the data, the background rate of  $^{116}\text{CdWO}_4$  detectors in the energy region 2.5–3.2 MeV ( $0\nu 2\beta$  decay energy of  $^{116}\text{Cd}$  is 2.8 MeV) was reduced to 0.04 counts/yr kg keV. It is the lowest background which has ever been reached with crystal scintillators.

<sup>4</sup> The same technique was applied to the sequence of decays from the  $^{235}\text{U}$  and  $^{238}\text{U}$  families. Activity of 5.5(14)  $\mu\text{Bq/kg}$  for  $^{227}\text{Ac}$  ( $^{235}\text{U}$  family) and limit  $\leq 4$   $\mu\text{Bq/kg}$  for  $^{226}\text{Ra}$  ( $^{238}\text{U}$  family) in the  $^{116}\text{CdWO}_4$  crystals were set.

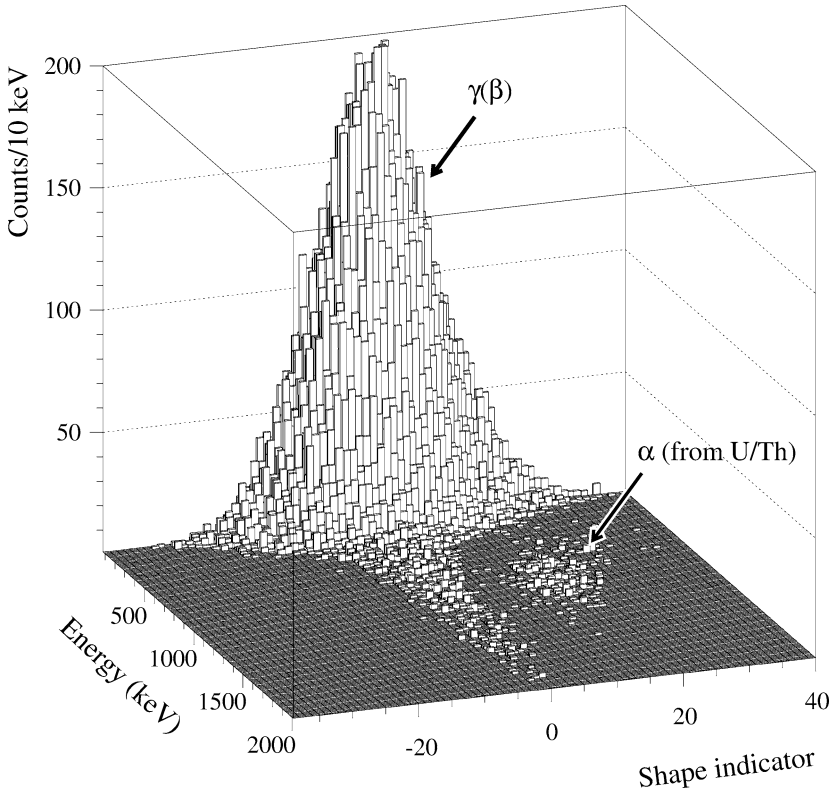


Fig. 5. Three-dimensional distribution of the background events (692 h of exposure with the PSA threshold of 80 keV) versus energy and shape indicator. The population of  $\alpha$  events belonging to the U/Th families is clearly separated from  $\gamma(\beta)$  background.

### 3. Results and discussion

#### 3.1. Background interpretation

The energy spectrum of the  $\gamma(\beta)$  events measured during 13316 h of live time in the low background set-up with the  $^{116}\text{CdWO}_4$  crystal scintillators (and selected by the PSA) is shown in Fig. 6. In the low energy region the background is caused mainly by the fourth-forbidden  $\beta$  decay of  $^{113}\text{Cd}$  ( $T_{1/2} = 7.7 \times 10^{15}$  yr [27],  $Q_\beta = 316$  keV) and  $\beta$  decay of  $^{113\text{m}}\text{Cd}$  ( $T_{1/2} = 14.1$  yr,  $Q_\beta = 580$  keV [28]).<sup>5</sup> The distribution above  $\approx 0.5$  MeV is described by the  $2\nu 2\beta$  decay spectrum of  $^{116}\text{Cd}$  with  $T_{1/2} = 2.9 \times 10^{19}$  yr (see below), trace contamination of the enriched and shield crystals by  $^{137}\text{Cs}$  and  $^{40}\text{K}$ , and external  $\gamma$  rays. The energy distributions for the above mentioned background

<sup>5</sup> Abundance of  $^{113}\text{Cd}$  in the enriched crystals was measured with the help of mass-spectrometer as  $\delta = 2.15(20)\%$  [29]. The possible presence of  $^{113\text{m}}\text{Cd}$  in the  $\text{CdWO}_4$  scintillators was confirmed by the low background measurements with two crystals, where  $\beta$  spectrum of  $^{113\text{m}}\text{Cd}$  was observed surely [30].



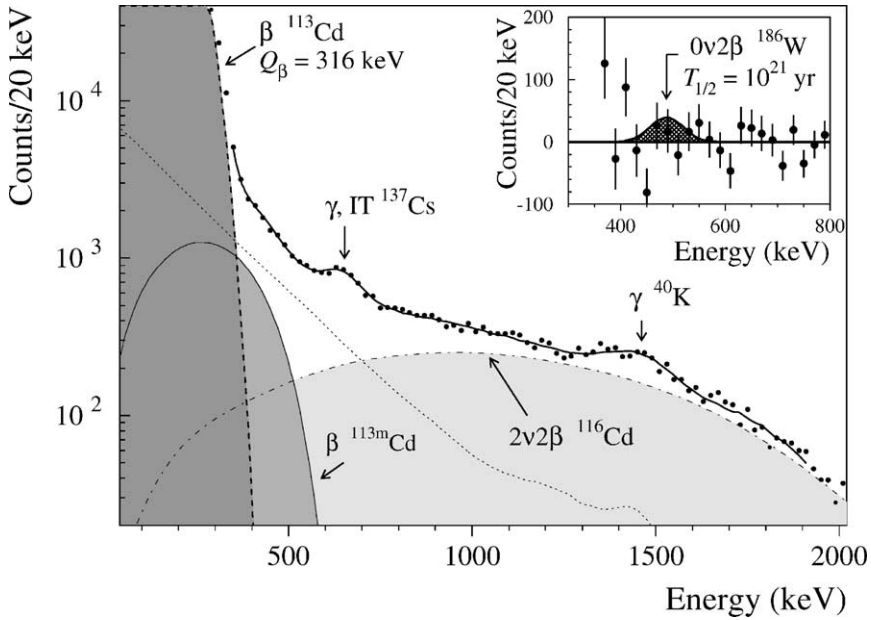


Fig. 6. Spectrum of  $\gamma(\beta)$  events measured with  $^{116}\text{CdWO}_4$  detectors during 13316 h and selected by the pulse shape analysis. Solid line represents the fit of the data in 340–1900 keV energy interval. Also shown are the most important components of the background:  $\beta$  spectra of  $^{113}\text{Cd}$  and  $^{113\text{m}}\text{Cd}$ ,  $2\nu 2\beta$  spectrum of  $^{116}\text{Cd}$  with  $T_{1/2}^{2\nu} = 2.9 \times 10^{19}$  yr, and model distribution of external  $\gamma$ s (dashed line). (Inset) The difference between experimental data and fit in the energy region of the  $0\nu 2\beta$  decay of  $^{186}\text{W}$ . The shadowed peak is the excluded at 90% C.L. effect corresponding to  $0\nu 2\beta$  decay of  $^{186}\text{W}$  with  $T_{1/2} = 10^{21}$  yr.

components were simulated with the help of the code GEANT3.21 and event generator DECAY4. The best least squares fit ( $\chi^2/\text{n.d.f.} = 1.3$ ) of the experimental spectrum in the 0.34–1.9 MeV energy interval by the sum of the listed components (to describe external  $\gamma$ -s the exponential function was used in addition to the  $^{40}\text{K}$ ,  $^{232}\text{Th}$  and  $^{238}\text{U}$  contamination of the PMTs, whose activities were previously measured [31]) gives the intrinsic activities (mBq/kg) of the  $^{116}\text{CdWO}_4$  crystals: 1.1(1) for  $^{113\text{m}}\text{Cd}$ , 0.43(6) for  $^{137}\text{Cs}$ , and 0.3(1) for  $^{40}\text{K}$ . The contamination of the natural  $\text{CdWO}_4$  crystals by  $^{40}\text{K}$  was calculated as 1.5(3) mBq/kg. The fitting curve and main components of the background are presented in Fig. 6.

Besides, the fit was repeated with the described model, into which other  $\beta(\gamma)$ -active impurities were included:  $^{210}\text{Pb}$ ,  $^{234\text{m}}\text{Pa}$  ( $^{238}\text{U}$  family),  $^{228}\text{Ac}$  ( $^{232}\text{Th}$ ),  $^{90}\text{Sr}$  (in equilibrium with  $^{90}\text{Y}$ ). However, only limits on their activities in the  $^{116}\text{CdWO}_4$  scintillators were obtained, as follows:  $^{210}\text{Pb} \leq 0.4$  mBq/kg,  $^{234\text{m}}\text{Pa} \leq 0.2$  mBq/kg,  $^{228}\text{Ac} \leq 0.1$  mBq/kg,  $^{90}\text{Sr} \leq 0.2$  mBq/kg.

The lowest energy part of the experimental spectrum is dominated by the  $\beta$  spectrum of  $^{113}\text{Cd}$ . To determine its activity, the background of the  $^{116}\text{CdWO}_4$  detectors was measured during 692 h with the energy threshold of 80 keV, which allows us to extend the PSA technique to this energy region. Fitting the data by sum of the simulated  $\beta$  spectra of  $^{113}\text{Cd}$  and exponential function (to describe residual background) we estimate the activity

of  $^{113}\text{Cd}$  in the enriched crystals as 91(5) mBq/kg. It corresponds to the abundance of this isotope in the detector  $\delta = 1.99(10)\%$ , that is in agreement with the result of mass-spectrometric measurement  $\delta = 2.15(20)\%$  [29]. The background rate in the energy interval 100–160 keV (where the peaks of double electron capture in  $^{180}\text{W}$  are expected) is equal to 45.4(3) counts/(day keV kg). Hence, we can conclude that at least 90% of events in this interval are caused by decays of  $^{113}\text{Cd}$ , and only residual 10% are attributed to above described sources of background, mainly to the external  $\gamma$  rays and  $\beta$  decay of  $^{113\text{m}}\text{Cd}$ .

### 3.2. Two-neutrino double beta decay of $^{116}\text{Cd}$

Earlier, after 4629 h of data taking in our experiment, the preliminary half-life value of two-neutrino  $2\beta$  decay of  $^{116}\text{Cd}$  was reported as  $T_{1/2}^{2\nu} = 2.6 \pm 0.1(\text{stat})_{-0.4}^{+0.7}(\text{syst}) \times 10^{19}$  yr [13]. In the present work with aim to derive the refined  $T_{1/2}^{2\nu}$  value and the shape of  $2\nu 2\beta$  decay spectrum of  $^{116}\text{Cd}$ , we are using the advantage of higher statistics collected during 12649 h after the last upgrading of the set-up in 1999, when spectrometric parameters of the detector (in particular, the energy resolution and pulse shape discrimination ability) were improved. The  $^{116}\text{CdWO}_4$  crystals contain  $4.54 \times 10^{23}$  nuclei of  $^{116}\text{Cd}$ , thus, the product of this number and the measuring time is  $6.56 \times 10^{23}$  nuclei  $\times$  yr. The total efficiency to detect  $2\nu 2\beta$  decay of  $^{116}\text{Cd}$  by the  $^{116}\text{CdWO}_4$  crystals is estimated as 0.93 (Monte Carlo simulation gives the registration efficiency of the  $2\nu 2\beta$  decay events as 0.96, while the efficiency of PSA for selection of  $\gamma(\beta)$  events is 0.97).

The part of the experimental spectrum used for the data analysis is depicted in Fig. 7. The data in the energy interval 800–2800 keV were simulated with the help of the GEANT3.21 package and event generator DECAY4. In addition to the  $^{116}\text{Cd}$  two-neutrino  $2\beta$  decay distribution, only three background components were considered. These are  $^{40}\text{K}$  contamination of the enriched and natural  $\text{CdWO}_4$  scintillators and external  $\gamma$  background caused by  $^{40}\text{K}$ ,  $^{232}\text{Th}$  and  $^{238}\text{U}$  contamination of the PMTs (one PMT for  $^{116}\text{CdWO}_4$  and one PMT for  $\text{CdWO}_4$  crystals, and two PMTs for plastic active shield). The radioactive impurities of each PMT were previously measured by R&D low background set-up as 2–4 Bq/PMT for  $^{40}\text{K}$ , (0.4–2.2) and (0.1–0.2) Bq/PMT for  $^{226}\text{Ra}$  and  $^{228}\text{Th}$  activity, respectively [31].

The fit of experimental data was carried out for different energy intervals in the range (800–1500)–(2000–2800) keV. Best fit ( $\chi^2/\text{n.d.f.} = 0.74$ ), achieved in the energy interval 860–2700 keV, gives the following results: the activities of  $^{40}\text{K}$  inside the enriched and natural  $\text{CdWO}_4$  crystals are equal to 0.4(2) and 1.6(4) mBq/kg, respectively; the half-life value of the  $2\nu 2\beta$  decay of  $^{116}\text{Cd}$  is  $2.9 \pm 0.06(\text{stat}) \times 10^{19}$  yr (the corresponding activity is about 1 mBq/kg).

In addition, we have justified our model with the help of experimental  $2\nu 2\beta$  decay Kurie plot:  $K(\varepsilon) = [S(\varepsilon)/\{\varepsilon^4 + 10\varepsilon^3 + 40\varepsilon^2 + 60\varepsilon + 30\}\varepsilon]^{1/5}$ , where  $S$  is the number of events with the energy  $\varepsilon$  (in units of electron mass) in the experimental spectrum after background subtraction. For the true  $2\nu 2\beta$  decay events such a Kurie plot should be the straight line  $K(\varepsilon) \sim (Q_{2\beta} - \varepsilon)$ . The obtained experimental Kurie plot is depicted in the inset of Fig. 7,

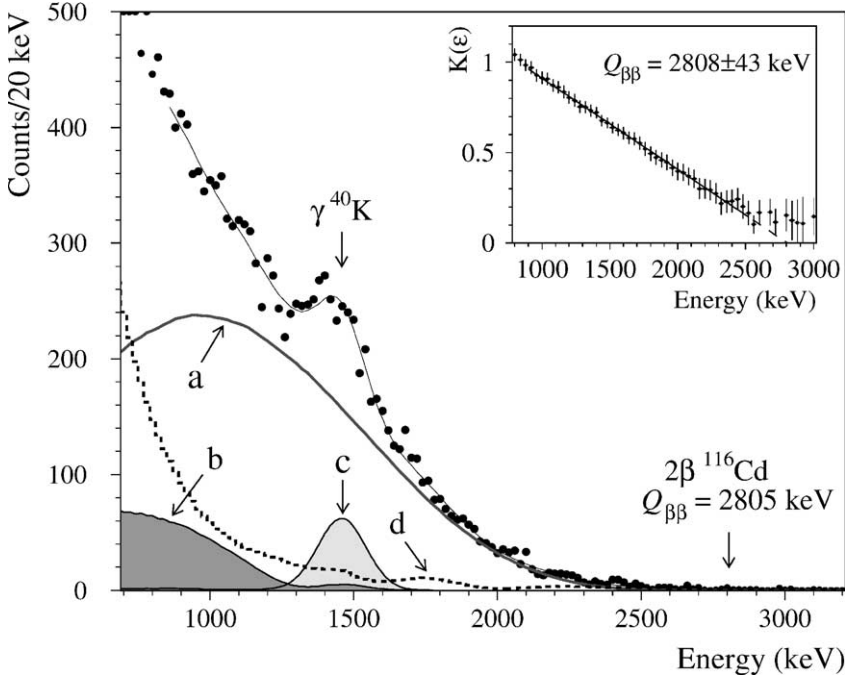


Fig. 7. The part of  $\gamma(\beta)$  spectrum measured with  $^{116}\text{CdWO}_4$  detectors during 12649 h, which was used for the determination of the half-life of  $2\nu 2\beta$  decay of  $^{116}\text{Cd}$ . Also shown are the most important model components: (a) the  $2\nu 2\beta$  spectrum of  $^{116}\text{Cd}$ ;  $^{40}\text{K}$  contamination of the enriched (b) and natural (c)  $\text{CdWO}_4$  scintillators; (d) external  $\gamma$  background caused by  $^{40}\text{K}$ ,  $^{232}\text{Th}$  and  $^{238}\text{U}$  contamination of the PMTs. Solid line represents the fit of the data in the 860–2700 keV energy interval. (Inset) The  $2\nu 2\beta$  decay Kurie plot and its fit by the straight line in the 900–2500 keV energy region.

from which one can see that in the energy region 0.9–2.5 MeV it is indeed well fitted by the straight line with  $Q_{2\beta} = 2808(43)$  keV (table value is  $Q_{2\beta} = 2805(4)$  keV).<sup>6</sup>

It should be stressed that statistics collected in our experiment (9850 events of  $2\nu 2\beta$  decay of  $^{116}\text{Cd}$  within the energy interval 800–2800 keV) and a signal to background ratio (3 : 1 for the energy interval 1.2–2.8 MeV, and 8 : 1 for the energy range 1.9–2.2 MeV) are among the highest ones reached up-to-date in  $2\beta$  decay experiments [5–7].

Different origins of systematical uncertainties of the measured half-life were taken into account (see Table I in Ref. [13]). The main ones are possible trace of the  $\beta$  active nuclides: ( $^{234\text{m}}\text{Pa}$  and  $^{90}\text{Sr}$  in equilibrium with  $^{90}\text{Y}$ ) in the  $^{116}\text{CdWO}_4$  crystals. From the upper limit on  $^{226}\text{Ra}$  contamination, derived with the help of time-amplitude analysis of data, it is obtained that activity of  $^{238}\text{U}$  (and, therefore, of  $^{234\text{m}}\text{Pa}$ ) in the enriched crystals is less

<sup>6</sup> To take into account the energy resolution of the detector, the fitting procedure was repeated by using the convolution of the theoretical  $2\nu 2\beta$  distribution  $\rho(\epsilon) = A \cdot \epsilon(\epsilon^4 + 10\epsilon^3 + 40\epsilon^2 + 60\epsilon + 30) \cdot (Q_{2\beta} - \epsilon)^5$  with the detector resolution function ( $A$ , which is inverse proportional to  $T_{1/2}^{2\nu}$ , and  $Q_{2\beta}$  were taken as free parameters). The fit in the energy region 1.2–2.8 MeV yields a very similar  $Q_{2\beta}$  and half-life values.

than 0.7 mBq/kg.<sup>7</sup> To estimate a systematic uncertainties, both  $\beta$  nuclides ( $^{234\text{m}}\text{Pa}$  and  $^{90}\text{Sr}$ – $^{90}\text{Y}$ ) were included in the fitting procedure, which leads to the stronger bound on their total activity  $\leq 0.3$  mBq/kg.

The final half-life value is equal to:  $T_{1/2}^{2\nu} = 2.9 \pm 0.06(\text{stat})_{-0.3}^{+0.4}(\text{syst}) \times 10^{19}$  yr. This value is in an agreement with our preliminary result  $T_{1/2}^{2\nu} = 2.6 \pm 0.1(\text{stat})_{-0.4}^{+0.7}(\text{syst}) \times 10^{19}$  yr [13], and with those measured earlier:  $T_{1/2}^{2\nu} = 2.6_{-0.5}^{+0.9} \times 10^{19}$  yr [33],  $T_{1/2}^{2\nu} = 2.7_{-0.4}^{+0.5}(\text{stat})_{-0.6}^{+0.9}(\text{syst}) \times 10^{19}$  yr [34], and  $T_{1/2}^{2\nu} = 3.75 \pm 0.35(\text{stat}) \pm 0.21(\text{syst}) \times 10^{19}$  yr [35].

### 3.3. Double beta decay of $^{186}\text{W}$

The background spectrum of Fig. 6 was used to search for neutrinoless  $2\beta$  decay of  $^{186}\text{W}$  to the ground state or to the first excited ( $2^+$ ) level of  $^{186}\text{Os}$ . The counting rate in the energy range of interest (440–540 keV) is equal to 0.333(4) counts/(day keV kg). In the experimental data there are no indications for the positive signals searched for, hence, we can only put the limits on their probabilities with the help of the known formula:  $\lim T_{1/2} = N \cdot \ln 2 \cdot \eta \cdot t / \lim S$ , where  $N$  is the number of  $^{186}\text{W}$  nuclei ( $1.56 \times 10^{23}$ ),  $\eta$  is the total detection efficiency,  $t$  is the measuring time (13316 h), and  $\lim S$  is the number of effect's events, which can be excluded at a given confidence level. The total detection efficiency includes the efficiency of registration of the  $0\nu 2\beta$  decay events by the  $^{116}\text{CdWO}_4$  scintillators ( $\eta_R$ ), and the efficiency of the PSA for selection of  $\gamma(\beta)$  events ( $\eta_{\text{PSA}}$ ). The first value was determined by the Monte Carlo simulation (see Fig. 2(b)) as  $\eta_R = 99.4\%$ , thus, taking into account the PSA efficiency ( $\eta_{\text{PSA}} = 95\%$ ), the total efficiency is  $\eta = 94\%$ .

The values of  $\lim S$  were determined in two ways. First, it was estimated simply as square root of the number of background counts in the energy window of interest. Notwithstanding its simplicity this method gives the right scale of the sensitivity of the experiment. In the energy interval 440–540 keV, which contains 89% of the expected  $0\nu 2\beta$  peak (so, the total efficiency  $\eta = 84\%$ ), there are 6091 counts, hence, the square root estimate gives  $\lim S = 128$  counts at 90% C.L. Using this value, we obtain the half-life limit  $T_{1/2} \geq 1.1 \times 10^{21}$  yr at 90% C.L. Secondly, the  $\lim S$  was determined by using the standard least squares procedure, where the experimental spectrum in the 380–1200 keV energy interval was fitted by the sum of the  $0\nu 2\beta$  decay peak being sought and background components determined above ( $^{113\text{m}}\text{Cd}$ ,  $^{137}\text{Cs}$ , exponential as external  $\gamma$  rays and  $2\nu 2\beta$  decay of  $^{116}\text{Cd}$ ). The fit ( $\chi^2/\text{n.d.f.} = 1.06$ ) yields the peak area ( $-21 \pm 95$ ) counts, that is no evidence for the effect. Conservatively treating such a negative difference as zero, one can get  $\lim S = 156$  (95) counts at 90% (68%) C.L. Using these values and the total efficiency  $\eta = 94\%$ , we set the following half-life limit on the  $0\nu 2\beta$  decay of  $^{186}\text{W}$  to the ground level of  $^{186}\text{Os}$ :

$$T_{1/2}^{0\nu}(^{186}\text{W}) \geq 1.0 (1.6) \times 10^{21} \text{ yr} \quad \text{at 90\% (68\%) C.L.}$$

<sup>7</sup> Analysis of alpha spectra [32] gives the similar estimation ( $\leq 0.6$  mBq/kg) for total activity of  $^{238}\text{U}$  and  $^{234}\text{U}$ .

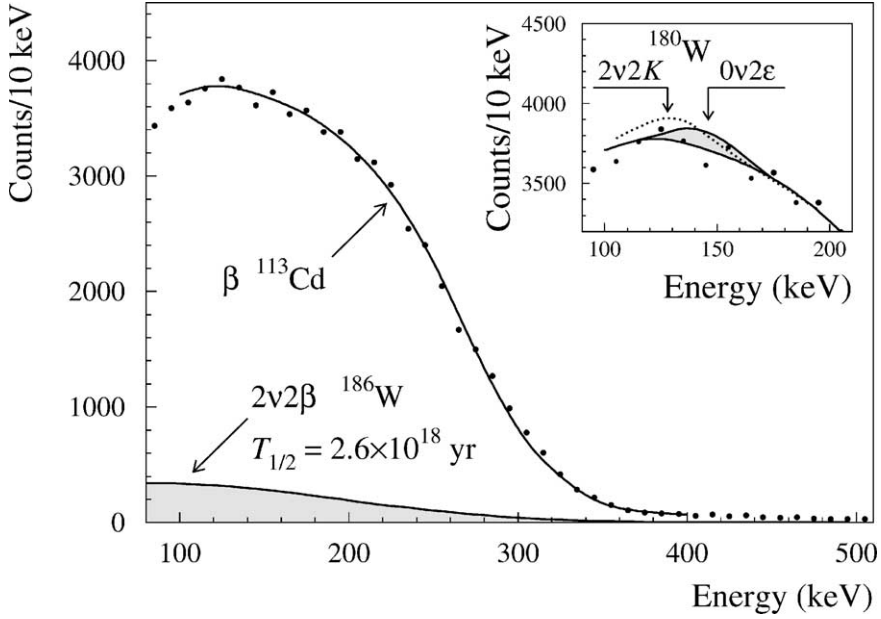


Fig. 8. Low energy part of the spectrum measured during 692 h by the  $^{116}\text{CdWO}_4$  detectors with the energy threshold of 80 keV (the  $\gamma(\beta)$  events were selected by the PSA with efficiency of 98%). The fitting curve is drawn by the solid line. Shaded distribution is  $2\nu 2\beta$  decay spectrum of  $^{186}\text{W}$  with  $T_{1/2}^{2\nu} = 2.6 \times 10^{18}$  yr excluded at 90% C.L. (Inset) The part of the spectrum together with the  $2\nu 2K$  peak of  $^{180}\text{W}$  with  $T_{1/2}^{2\nu 2K} = 0.7 \times 10^{17}$  yr (dotted line) and  $0\nu 2\varepsilon$  peak of  $^{180}\text{W}$  with  $T_{1/2}^{0\nu 2\varepsilon} = 0.9 \times 10^{17}$  yr (shaded), both excluded at 90% C.L.

In the inset of Fig. 6 the difference between the experimental and model spectra is shown together with the excluded peak of the  $0\nu 2\beta$  decay of  $^{186}\text{W}$ .

In case of the  $0\nu 2\beta$  decay of  $^{186}\text{W}$  to the first excited ( $2^+$ ) level of  $^{186}\text{Os}$ , the  $\gamma$  quanta with the energy of 137 keV (deexcitation of the  $2^+$  level of  $^{186}\text{Os}$ ) will be emitted. Due to practically full absorption of these  $\gamma$  quanta by the  $^{116}\text{CdWO}_4$  crystals, the expected response function does not differ from that for transition to ground state (see Fig. 2(b)). The total efficiency is equal to  $\eta = 92\%$ , which leads to the same half-life limit:

$$T_{1/2}^{0\nu}({}^{186}\text{W, g.s.} \rightarrow 2^+) \geq 1.0 (1.6) \times 10^{21} \text{ yr} \quad \text{at 90\% (68\%) C.L.}$$

Similarly, for the  $0\nu 2\beta$  decay of  $^{186}\text{W}$  with emission of Majoron, fit of the spectrum gives the following restriction for the half-life:

$$T_{1/2}^{0\nu M}({}^{186}\text{W}) \geq 1.2 (1.4) \times 10^{20} \text{ yr} \quad \text{at 90\% (68\%) C.L.}$$

To estimate lower limit for the  $2\nu 2\beta$  decay of  $^{186}\text{W}$ , we have considered the background spectrum accumulated during 692 h with the low energy threshold (Fig. 8). Only 2% of  $\gamma(\beta)$  events have been removed from the data as result of the PSA ( $\eta_{\text{PSA}} = 98\%$ ). Because practically 100% of beta particles from expected  $2\nu 2\beta$  decay are absorbed in the crystals, the total efficiency is  $\eta = 98\%$ . The simple model (it includes the  $2\nu 2\beta$  spectrum of  $^{186}\text{W}$ ,  $\beta$  spectrum of  $^{113}\text{Cd}$  and exponential function) was used to fit the experimental data. The

best fit ( $\chi^2/\text{n.d.f.} = 1.9$ ), achieved in the energy interval 100–500 keV, gives  $60 \pm 1962$  events for the effect searched for. It yields 3277 (2022) counts excluded at 90% (68%) C.L., and consequently, the following half-life limit for the  $2\nu 2\beta$  decay of  $^{186}\text{W}$ :

$$T_{1/2}^{2\nu}({}^{186}\text{W}) \geq 2.6 (4.1) \times 10^{18} \text{ yr} \quad \text{at 90\% (68\%) C.L.}$$

The  $2\nu 2\beta$  decay distribution of  $^{186}\text{W}$  excluded at 90% C.L. is depicted in Fig. 8.

The same method gives the bound for  $2\nu 2\beta$  transition to the first ( $2^+$ ) excited level of  $^{186}\text{Os}$ :

$$T_{1/2}^{2\nu}({}^{186}\text{W, g.s.} \rightarrow 2^+) \geq 1.0 (1.3) \times 10^{19} \text{ yr} \quad \text{at 90\% (68\%) C.L.}$$

### 3.4. Double electron capture in $^{180}\text{W}$

To set the limits on the  $0\nu 2\varepsilon$  process in  $^{180}\text{W}$ , the background spectrum of  $^{116}\text{CdWO}_4$  detector measured during 692 h with the low energy threshold (see Fig. 8) was used. The least squares fit of this spectrum in the 90–240 keV energy interval gives  $91 \pm 177$  counts for the peak searched for ( $\chi^2/\text{n.d.f.} = 1.3$ ), that is no evidence for the effect. These numbers lead to an upper limit of 381 (268) counts at 90% (68%) C.L. Taking into account 100% registration efficiency for this process (thus, the total efficiency  $\eta = \eta_{\text{PSA}} = 98\%$ ) and number of  $^{180}\text{W}$  nuclei ( $6.57 \times 10^{20}$ ), one can calculate the half-life limit:

$$T_{1/2}^{0\nu 2\varepsilon}({}^{180}\text{W}) \geq 0.9 (1.3) \times 10^{17} \text{ yr} \quad \text{at 90\% (68\%) C.L.}$$

The same method gives the restriction for the  $2\nu 2K$  process in  $^{180}\text{W}$ :

$$T_{1/2}^{2\nu 2K}({}^{180}\text{W}) \geq 0.7 (0.8) \times 10^{17} \text{ yr} \quad \text{at 90\% (68\%) C.L.}$$

The peaks of the  $0\nu 2\varepsilon$  and  $2\nu 2K$  of  $^{180}\text{W}$  excluded at 90% C.L. are shown in the inset of Fig. 8.

## 4. Conclusions

With the help of the super-low background  $^{116}\text{CdWO}_4$  scintillators the refined half-life value of the two-neutrino  $2\beta$  decay of  $^{116}\text{Cd}$  is measured as:  $T_{1/2}^{2\nu} = 2.9 \pm 0.06(\text{stat})_{-0.3}^{+0.4}(\text{syst}) \times 10^{19}$  yr. The measured  $2\nu 2\beta$  Kurie plot is well described by the straight line, and derived  $Q_{\beta\beta}$  value ( $2808 \pm 43$  keV) is in accordance with the table value 2805(4) keV.

All half-life limits on  $2\beta$  decay processes in  $^{186}\text{W}$  and  $^{180}\text{W}$  obtained in the present experiment with the help of the low background  $^{116}\text{CdWO}_4$  scintillators are summarized in Table. Note that limit  $T_{1/2}^{0\nu} \geq 10^{21}$  yr on the  $0\nu 2\beta$  decay of  $^{186}\text{W}$  is near one order of magnitude higher than previous result [29], and that up to now such a level was reached only for ten nuclides [7]. The bounds for the  $0\nu$  decay with Majoron emission and for the  $2\nu$  decay to the first ( $2^+$ ) excited level of  $^{186}\text{Os}$  are set for the first time. However, obtained

Table 1  
Half-life limits on the  $2\beta$  decay processes in  $^{180}\text{W}$  and  $^{186}\text{W}$

Nuclide	Decay mode			Experimental $T_{1/2}$ limit, yr		
				Present work		[29] 90% C.L.
				90% C.L.	68% C.L.	
$^{180}\text{W}$	$2\epsilon$	$0\nu$	g.s.–g.s.	$0.9 \times 10^{17}$	$1.3 \times 10^{17}$	$0.5 \times 10^{17}$
	$2K$	$2\nu$	g.s.–g.s.	$0.7 \times 10^{17}$	$0.8 \times 10^{17}$	–
$^{186}\text{W}$	$2\beta^-$	$0\nu$	g.s.–g.s.	$1.0 \times 10^{21}$	$1.6 \times 10^{21}$	$2.7 \times 10^{20}$
			g.s.– $2^+$	$1.0 \times 10^{21}$	$1.6 \times 10^{21}$	$2.4 \times 10^{20}$
		$0\nu M$	g.s.–g.s.	$1.2 \times 10^{20}$	$1.4 \times 10^{20}$	–
		$2\nu$	g.s.–g.s.	$2.6 \times 10^{18}$	$4.1 \times 10^{18}$	$5.9 \times 10^{17}$
		$2\nu$	g.s.– $2^+$	$1.0 \times 10^{19}$	$1.3 \times 10^{19}$	–

results are still far from the theoretical predictions, which, e.g., for the  $0\nu 2\beta$  decay are in the range of  $6 \times 10^{24}$  yr [36]– $5 \times 10^{25}$  yr [37] (for  $m_\nu = 1$  eV).<sup>8</sup>

The half-life limits on the double electron capture of  $^{180}\text{W}$  established in our work are higher than those of previous experiment [29]. To date only five nuclei ( $^{40}\text{Ca}$ ,  $^{78}\text{Kr}$ ,  $^{106}\text{Cd}$ ,  $^{108}\text{Cd}$  and  $^{124}\text{Xe}$ ) were studied at the similar level of sensitivity [7].<sup>9</sup> However, these experimental bounds are still far from the theoretical prediction ( $\approx 10^{25}$  yr [39]), thus further efforts in this direction would be needed.

It is evident that sensitivity of the present experiment to double beta decay processes on tungsten isotopes is limited mainly by the background from the  $\beta$  decay of  $^{113}\text{Cd}$  ( $T_{1/2} = 7.7 \times 10^{15}$  yr,  $Q_\beta = 316$  keV, abundance in  $^{116}\text{CdWO}_4$  of  $\approx 2\%$ ),  $^{113\text{m}}\text{Cd}$  ( $T_{1/2} = 14.1$  yr,  $Q_\beta = 580$  keV), and from the  $2\nu 2\beta$  decay of  $^{116}\text{Cd}$  ( $T_{1/2}^{2\nu} = 2.9 \times 10^{19}$  yr). The latter can be substantially reduced by using non-enriched  $\text{CdWO}_4$  crystals (natural abundance of  $^{116}\text{Cd}$  is  $\approx 7.5\%$ ). However, in this case the background from the  $^{113}\text{Cd}$  and  $^{113\text{m}}\text{Cd}$  will be increased essentially because of high natural abundance of  $^{113}\text{Cd}$  ( $\delta \approx 12\%$ ). This difficulty could be overcome by replacing  $\text{CdWO}_4$  crystals with zinc ( $\text{ZnWO}_4$ ) or calcium ( $\text{CaWO}_4$ ) tungstate scintillators. Preliminary studies of the scintillation properties and radiopurity of these crystals gave us encouraging results both for  $\text{ZnWO}_4$  [40,41] and  $\text{CaWO}_4$  detectors.

Apparently, a higher sensitivity for such a research could be obtained by using  $\text{CdWO}_4$  ( $\text{ZnWO}_4$  or  $\text{CaWO}_4$ ) detectors enriched in  $^{180}\text{W}$  and  $^{186}\text{W}$ . Finally, let us mention an interesting possibility to exploit these crystals as low temperature bolometers [42,43], whose energy resolution is much better than that of scintillation detectors.

<sup>8</sup> It should be stressed that in accordance with theoretical calculations [36,37] the  $2\nu 2\beta$  decay rate of  $^{186}\text{W}$  is strongly suppressed as compared with those of other nuclei. Hence, the energy region of  $0\nu 2\beta$  signal of  $^{186}\text{W}$  will be free of the background created by the  $2\nu 2\beta$  events, which can reach this region due to the poor energy resolution of the detector [6,7]. The suppression of the  $2\nu$  mode would be especially important in the search for the  $0\nu$  decay with Majoron emission, whose distribution is continuous, because in this case the  $0\nu 2\beta M$  events will not be distinguished from the  $2\nu$  background even with the help of the high energy resolution detector.

<sup>9</sup> An indication on the existence of the  $2\beta^+$  decay processes in  $^{130}\text{Ba}$  and  $^{132}\text{Ba}$  was obtained in the geochemical measurements [38]; however, this result has to be confirmed by a direct counting experiment.

## References

- [1] Y. Fukuda, et al., Super-Kamiokande Collaboration, Phys. Rev. Lett. 81 (1998) 1562;  
Y. Fukuda, et al., Super-Kamiokande Collaboration, Phys. Rev. Lett. 82 (1999) 1810;  
Y. Fukuda, et al., Super-Kamiokande Collaboration, Phys. Rev. Lett. 82 (1999) 2430;  
Y. Fukuda, et al., Super-Kamiokande Collaboration, Phys. Rev. Lett. 86 (2001) 5651.
- [2] Q.R. Ahmad, et al., SNO Collaboration, Phys. Rev. Lett. 87 (2001) 071301;  
Q.R. Ahmad, et al., SNO Collaboration, Phys. Rev. Lett. 89 (2002) 011301;  
Q.R. Ahmad, et al., SNO Collaboration, Phys. Rev. Lett. 89 (2002) 011302.
- [3] C.K. Jung, K2K Collaboration, Int. J. Mod. Phys. A 17 (2002) 3364.
- [4] S.R. Elliot, P. Vogel, Annu. Rev. Nucl. Part. Sci. 52 (2002) 115.
- [5] J.D. Vergados, Phys. Rep. 361 (2002) 1.
- [6] Yu.G. Zdesenko, Rev. Mod. Phys. 74 (2002) 663.
- [7] V.I. Tretyak, Yu.G. Zdesenko, At. Data Nucl. Data Tables 80 (2002) 83.
- [8] R.K. Bardin, et al., Nucl. Phys. A 158 (1970) 337;  
V.B. Brudanin, et al., Phys. Lett. B 495 (2000) 63.
- [9] A.A. Klimenko, et al., Nucl. Instrum. Methods B 17 (1986) 445;  
A. De Silva, et al., Phys. Rev. C 56 (1997) 2451.
- [10] F.A. Danevich, et al., Nucl. Phys. A 694 (2001) 375.
- [11] S.R. Elliot, et al., Phys. Rev. C 46 (1992) 1535.
- [12] H. Ejiri, et al., Phys. Rev. C 63 (2001) 065501.
- [13] F.A. Danevich, et al., Phys. Rev. C 62 (2000) 045501;  
P.G. Bizzeti, et al., Nucl. Phys. B (Proc. Suppl.) 110 (2002) 389.
- [14] A. Alessandrello, et al., Phys. Lett. B 486 (2000) 13.
- [15] R. Luescher, et al., Phys. Lett. B 434 (1998) 407.
- [16] L. Baudis, et al., Phys. Rev. Lett. 83 (1999) 41.
- [17] C.E. Aalseth, et al., Phys. Rev. C 59 (1999) 2108;  
C.E. Aalseth, et al., Phys. Rev. D 65 (2002) 092007.
- [18] GEANT, CERN Program Library Long Write-up W5013, CERN, 1994.
- [19] O.A. Ponkratenko, et al., Phys. At. Nucl. 63 (2000) 1282.
- [20] K.J.R. Rosman, P.D.P. Taylor, Pure Appl. Chem. 70 (1998) 217.
- [21] G. Audi, A.H. Wapstra, Nucl. Phys. A 595 (1995) 409.
- [22] Yu.G. Zdesenko, et al., in: Proceedings 2nd International Symposium Underground Physics, Baksan Valley, USSR, August 17–19, 1987, Nauka, Moscow, 1988, p. 291.
- [23] P.G. Bizzeti, et al., Bull. Russ. Acad. Sci., Ser. Phys. 66 (2002) 630 (in Russian).
- [24] E. Gatti, F. De Martini, Nuclear Electronics 2, IAEA, Vienna, 1962, p. 265.
- [25] T. Fazzini, et al., Nucl. Instrum. Methods A 410 (1998) 213.
- [26] F.A. Danevich, et al., Nucl. Phys. A 694 (2001) 375.
- [27] F.A. Danevich, et al., Phys. At. Nucl. 59 (1996) 1.
- [28] R.B. Firestone, et al. (Eds.), Table of Isotopes, 8th Edition, Wiley, New York, 1996.
- [29] A.Sh. Georgadze, et al., Phys. At. Nucl. 58 (1995) 1093.
- [30] A.Sh. Georgadze, et al., Instrum. Exp. Tech. 39 (1996) 191.
- [31] F.A. Danevich, et al., Nucl. Phys. A 643 (1998) 317.
- [32] F.A. Danevich, et al., nucl-ex/0211013;  
F.A. Danevich, et al., Phys. Rev. C 67 (2003), in press.
- [33] H. Ejiri, et al., J. Phys. Soc. Jpn. 64 (1995) 339.
- [34] F.A. Danevich, et al., Phys. Lett. B 344 (1995) 72;  
A.Sh. Georgadze, et al., Phys. At. Nucl. 58 (1995) 1093.
- [35] R. Arnold, et al., Z. Phys. C 72 (1996) 239.
- [36] A. Staudt, et al., Europhys. Lett. 13 (1990) 535.
- [37] J.G. Hirsch, O. Castanos, P.O. Hess, Nucl. Phys. A 582 (1995) 124.
- [38] A.P. Meshik, et al., Phys. Rev. C 64 (2001) 035205.
- [39] Z. Sujkowski, S. Wycech, Acta Phys. Pol. B 33 (2002) 471.
- [40] F.A. Danevich, et al., Prib. Tekh. Eksp. 5 (1989) 80 (in Russian).



- [41] A.Sh. Georgadze, et al., *JETP Lett.* 61 (1995) 882.
- [42] A. Alessandrello, et al., *Nucl. Instrum. Methods A* 344 (1994) 243;  
A. Alessandrello, et al., *Nucl. Phys. B (Proc. Suppl.)* 35 (1994) 394.
- [43] M. Bravin, et al., *Astropart. Phys.* 12 (1999) 107.